Wavelets and Linear Algebra 4(1) (2017) 53 - 73

Vali-e-Asr University of Rafsanjan

Wavelets and Linear Algebra

http://wala.vru.ac.ir

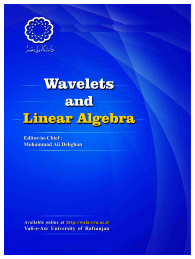

Wavelet-based numerical method for solving fractional integro-differential equation with a weakly singular kernel

Fakhrodin Mohammadi[a,*], Armando Ciancio[b]

[a]*Department of Mathematics, University of Hormozgan, P. O. Box 3995, Bandarabbas, Islamic Republic of Iran.*
[b]*Department of Biomedical Sciences and Morphological and Functional Imaging, University of Messina, via Consolare Valeria 1, 98125 MESSINA, Italy.*

Article Info

Article history:
Received 10 November 2016
Accepted 13 February 2017
Available online 01 July 2017
Communicated by Asghar Rahimi

Keywords:
Wavelet basis,
Collocation method,
Fractional integro-differential equation.

2000 MSC:
47G20, 45E05, 65L60.

Abstract

This paper describes and compares application of wavelet basis and Block-Pulse functions (BPFs) for solving fractional integro-differential equation (FIDE) with a weakly singular kernel. First, a collocation method based on Haar wavelets (HW), Legendre wavelet (LW), Chebyshev wavelets (CHW), second kind Chebyshev wavelets (SKCHW), Cos and Sin wavelets (CASW) and BPFs are presented for driving approximate solution FIDEs with a weakly singular kernel. Error estimates of all proposed numerical methods are given to test the convergence and accuracy of the method. A comparative study of accuracy and computational time for the presented techniques is given.

*Corresponding author
Email addresses: f.mohammadi62@hotmail.com (Fakhrodin Mohammadi), aciancio@unime.it (Armando

http://doi.org/10.22072/wala.2017.52567.1091

1. Introduction

Fractional calculus has been recently applied for modeling many physical phenomena in fields of nonlinear oscillation of earthquake, fluid-dynamic traffic, continuum and statistical mechanics, signal processing, control theory, and dynamics of interfaces between nanoparticles and subtracts [22, 2, 21, 20]. Consequently, considerable attentions has been given for deriving numerical solution of fractional functional equations. For example, Fourier transforms method, Laplace transforms method, fractional differential transform method, finite difference method, orthogonal functions, wavelets method, Adomian decomposition method, variational iteration method, and homotopy analysis method have been used for producing approximate solution of fractional functional equations[34, 32, 33, 31, 11, 9, 16].

Recently, different basis functions such as piecewise constant orthogonal functions, wavelets basis, orthogonal polynomials and Sine-Cosin functions have been used to estimate the solution of integral equations [26, 25**?** , 27, 4, 3, 5, 18, 19, 10, 15, 14]. FIDEs with a weakly singular kernel are used in modelling different physical processes. For example, these kind of integro-differential equations are used in the heat conduction problem, radiative equilibrium, elasticity and fracture mechanics [26, 25, 27, 13]. In this paper, we describe application of BPFs and wavelets basis in solving the FIDEs with a weakly singular kernel. Consider the FIDE with weakly singular kernel

$$D_*^{\alpha}u(t) = f(t) + \int_0^t \frac{u(s)ds}{(t-s)^{\beta}} + \int_0^1 k(s,t)u(s)ds, \tag{1.1}$$

with initial condition

$$u(0) = 0, \tag{1.2}$$

where $0 < \alpha, \beta < 1$, a and b are constants, $f(t)$ and $k(s,t)$ are known functions, u(t) is an unknown function and D_*^{α} denotes the fractional derivative defined by Caputo [22]. Operational matrices of fractional integration for BPFs and wavelets basis along with typical collocation method are used to obtain approximate solution of this FIDE with a weakly singular kernel. A comparison of the numerical results for different wavelets basis is presented.

The rest of this paper is organized as follows: In section 2 some preliminary definitions of fractional calculus are reviewed. Section 3 is devoted to the basic definitions of the BPFs and their properties. In section 4 we review definitions and properties of some commonly used wavelet basis in numerical solution of functional equations. A collocation method based on the wavelet and their operational matrix is proposed for solving fractional integro-differential equation with a weakly singular kernel is presented in Section 5. In Section 6 we introduce a process for estimating the error of approximate solution. A comparison of the numerical results is included in section 7. Finally, a conclusion is given in section 8.

2. Fractional calculus

Fractional order calculus is a branch of calculus which deal with integration and differentiation operators of non-integer order. Among the several formulations of the generalized derivative, the

Ciancio)

Riemann-Liouville and Caputo definition are the most commonly used. In this section we give some necessary definitions and mathematical preliminaries of the fractional calculus which are required for establishing our results.

Definition 2.1. A real function $f(t), t > 0$, is said to be in the space $C_\mu, \mu \in \mathbb{R}$ if there exists a real number $p > \mu$ and a function $f_1(t) \in C[0, \infty)$ such that $f(t) = t^p f_1(t)$, and it is said to be in the space $C_\mu^n,\ n \in \mathbb{N}$ if $f^{(n)} \in C_\mu$.

Definition 2.2. The Riemann-Liouville fractional integration of order $\alpha \geq 0$ of a function $f \in C_\mu, \mu \geq -1$, is defined as

$$(J^\alpha f)(t) = \begin{cases} \frac{1}{\Gamma(\alpha)} \int_0^t (t-\tau)^{\alpha-1} f(\tau) d\tau, & \alpha > 0, \\ f(t), & \alpha = 0. \end{cases} \tag{2.1}$$

The Riemann-Liouville fractional operator J^α has the following properties:

(a) $J^\alpha \left(J^\beta f(t)\right) = J^\beta \left(J^\alpha f(t)\right)$,

(b) $J^\alpha \left(J^\beta f(t)\right) = J^{\alpha+\beta} f(t)$,

(c) $J^\alpha t^\nu = \frac{\Gamma(\nu+1)}{\Gamma(\alpha+\nu+1)} t^{\nu+\alpha}, \alpha, \beta \geq 0, \nu > -1$.

Definition 2.3. Riemann-Liouville fractional derivative of order $\alpha > 0$ is defined as

$$D^\alpha f(t) = \frac{d^n}{dt^n} J^{n-\alpha} f(t), \qquad n \in \mathbb{N},\ \ n-1 < \alpha \leq n. \tag{2.2}$$

The Riemann-Liouville derivatives have certain disadvantages when trying to model real-world phenomena with fractional differential equations. Therefore, a modified fractional differential operator D_*^α was proposed by Caputo [22].

Definition 2.4. The fractional derivative of order $\alpha > 0$ in the Caputo sense is defined as

$$D_*^\alpha f(t) = \begin{cases} \frac{d^n f(t)}{dt^n}, & \alpha = n \in \mathbb{N}, \\ \frac{1}{\Gamma(n-\alpha)} \int_0^t \frac{f^{(n)}(\tau)}{(t-\tau)^{\alpha-n+1}} d\tau,\ t > 0, & 0 \leq n-1 < \alpha < n. \end{cases} \tag{2.3}$$

where n is an integer, $t > 0$, and $f \in C_1^n$.

Some useful relation between the Riemann-Liouvill and Caputo fractional operators is given by the following expression:

(a) $J^\alpha D_*^\alpha f(t) = f(t) - \sum_{k=0}^{n-1} f^{(k)}(0^+) \frac{t^k}{k!}, \quad n-1 < \alpha \leq n,\ \ t > 0$.

(b) $D_*^\alpha J^\alpha f(t) = f(t)$.

(c) $J^\alpha t^\beta = \frac{\Gamma(\beta+1)}{\Gamma(\beta-\alpha+1)} t^{\beta-\alpha}$.

(d) $D_*^\alpha t^\beta = \begin{cases} \frac{\Gamma(\beta+1)}{\Gamma(\beta-\alpha+1)} t^{\beta-\alpha} & \beta \geq \alpha, \\ 0 & \beta < \alpha. \end{cases}$

For more details about fractional calculus please see [22].

3. Block pulse functions (BPFs)

BPFs have been studied by many authors and also have been applied for solving different problems. Here, we present a brief review of BPFs and its properties [9, 11].

The m-set of BPFs are defined as

$$b_i(t) = \begin{cases} 1 & (i-1)h \leq t < ih \\ 0 & otherwise \end{cases} \tag{3.1}$$

in which $t \in [0, T)$, $i = 1, 2, ..., m$ and $h = \frac{T}{m}$. The BPFs set are disjoint with each other in the interval $[0, T)$ and

$$b_i(t)b_j(t) = \delta_{ij}b_i(t), \quad i, j = 1, 2, ..., m, \tag{3.2}$$

where δ_{ij} is the Kronecker delta. The set of BPFs defined in the interval $[0, T)$ are orthogonal with each other, that is

$$\int_0^T b_i(t)b_j(t)dt = h\delta_{ij}, \quad i, j = 1, 2, ..., m. \tag{3.3}$$

As m tends to infinity, the m-set BPFs becomes a complete basis for $L^2[0, T)$, so that an arbitrary real bounded function $f(t)$, which is square integrable in the interval $[0, T)$, can be expanded into a BPFs series as

$$\int_0^T f^2(t)dt = \sum_{i=1}^{\infty} f_i^2 \|b_i(t)\|^2, \tag{3.4}$$

where

$$f_i = \frac{1}{h}\int_0^T b_i(t)f(t)dt. \tag{3.5}$$

Any absolutely integrable function $f(t)$ defined over $[0, T)$ can be approximated by using BPFs as

$$f(t) \simeq f_m(t) = \sum_{i=1}^{m} f_i b_i(t) = F^T B(t), \tag{3.6}$$

in which f_i is obtained in (3.5), $B(t)$ and F are m-vectors given by

$$B(t) = [b_1(t), ..., b_m(t)]^T, \tag{3.7}$$

$$F = [f_1, f_2, ..., f_m]^T. \tag{3.8}$$

Also the BPFs coefficients f_i are obtained as (3.5), such that the mean square error between $f(t)$ and its BPFs expansion (3.6) in the interval of $t \in [0, T)$ is minimal. Morever, any two dimensional function $k(s, t) \in L^2([0, T] \times [0, T])$ can be expanded with respect to BPFs such as

$$k(s, t) \simeq B(t)^T \Pi B(t),$$

where $B(t)$ is the m-dimensional BPFs vectors respectively, and Π is the $m \times m$ BPFs coefficient matrix with (i, j)-th element

$$\Pi_{ij} = \frac{1}{h^2} \int_0^T \int_0^T k(s,t) b_i(t) b_j(s) dt ds, \quad i, j = 1, 2, ..., m,$$

and $h = \frac{T}{m}$.

3.1. BPFs operational matrices

Kilicman and Al Zhour [12] investigated the generalized integral operational matrix and showed that the integral of the matrix $B(t)$ defined in (3.7), can be approximated by

$$\int_0^t B(\tau) d\tau \simeq PB(t), \tag{3.9}$$

where P is the $m \times m$ operational matrix of one-time integral of $B(t)$. Moreover, we can compute the generalized operational matrices P^n of n-times integration of $B(t)$ as:

$$\underbrace{\int_0^t \cdots \int_0^t}_{n-times} B(\tau)(d\tau)^n \simeq P^n B(t). \tag{3.10}$$

In [12] it is shown that P^n has the following form:

$$P^n = \frac{h^n}{(n+1)!} \begin{pmatrix} 1 & \xi_1 & \xi_2 & \dots & \xi_{m-1} \\ 0 & 1 & \xi_1 & \dots & \xi_{m-2} \\ 0 & 0 & 1 & \dots & \xi_{m-3} \\ 0 & 0 & 0 & \ddots & \vdots \\ 0 & 0 & 0 & 0 & 1 \end{pmatrix}, \tag{3.11}$$

where $\xi_i = (i+1)^{n+1} - 2i^{n+1} + (i-1)^{n+1}$. As a generalization of the operational matrix P, the BPFs operational matrix of fractional integration is defined as

$$J^\alpha B(t) = P^\alpha B(t), \tag{3.12}$$

where P^α is the $m \times m$ operational matrix of fractional integration and

$$P^\alpha = \frac{h^\alpha}{\Gamma(\alpha+2)} \begin{pmatrix} 1 & \xi_1 & \xi_2 & \dots & \xi_{m-1} \\ 0 & 1 & \xi_1 & \dots & \xi_{m-2} \\ 0 & 0 & 1 & \dots & \xi_{m-3} \\ 0 & 0 & 0 & \ddots & \vdots \\ 0 & 0 & 0 & 0 & 1 \end{pmatrix}, \tag{3.13}$$

and $\xi_i = (i+1)^{\alpha+1} - 2i^{\alpha+1} + (i-1)^{\alpha+1}$. A detailed procedure for computing the operational matrix P^α can be found in [12].

4. Multiresolution analysis and wavelets

A multiresolution analysis (MRA) of $L^2(\mathbb{R})$ is defined as a sequence of closed subspaces V_j of $L^2(\mathbb{R})$, $j \in \mathbb{Z}$, with the following properties [7, 8]:
(1) $V_j \subset V_{j+1}$,
(2) $v(x) \in V_j \iff v(2x) \in V_{j+1}$,
(3) $v(x) \in V_0 \iff v(x+1) \in V_0$,
(4) $\bigcup_{j=-\infty}^{\infty} V_j$ is dense in $L^2(\mathbb{R})$ and $\bigcap_{j=-\infty}^{\infty} V_j = 0$,
(5) There exists a scaling function $\varphi(x) \in V_0$, such that the set $\{\varphi(x-k), k \in \mathbb{Z}\}$ forms a Riesz basis of V_0.
The function $\varphi(x)$ whose existence is asserted in (5) is called a scaling function of the given MRA. Moreover, a Riesz basis for a separable Hilbert space H is a basis $\{g_n\}$ that is close to being orthogonal. That is, there exists a bounded invertible operator which maps $\{g_n\}$ onto an orthonormal basis. Any function $f \in L^2(\mathbb{R})$ can be projected onto the space V_n by means of a projection operator $P_n f(t)$, as follows:

$$P_n f(t) = \sum_k a_{j,k} \varphi\left(2^j t - k\right). \tag{4.1}$$

A set of orthonormal wavelets can be constructed by using an MRA. Let W_0 be the orthogonal complement of V_0 in V_1; that is, $V_1 = V_0 \oplus W_0$. Then, if we dilate the elements of W_0 by 2^j we obtain a closed subspace V_j in V_{j+1} such that

$$V_{j+1} = V_j \oplus W_j. \tag{4.2}$$

Since $V_j \to 0$ as $j \to -\infty$ and $V_j \to L^2(\mathbb{R})$ as $j \to \infty$, we have

$$V_{j+1} = V_j \oplus W_j = \bigoplus_{r=-\infty}^{j} W_r, \tag{4.3}$$

and

$$L^2(\mathbb{R}) = \bigoplus_{j=-\infty}^{\infty} W_j. \tag{4.4}$$

Therefore, to find an orthonormal wavelets basis, we need to find a function ψ in W_0 such that $\{\psi(t-k), k \in \mathbb{Z}\}$ is an orthonormal basis for W_0. In this case, the set $\left\{2^{\frac{j}{2}}\psi(2^j t - k), k \in \mathbb{Z}\right\}$ is an orthonormal basis for W_j. Consequently, the set $\left\{\psi_{j,k}(t) = 2^{\frac{j}{2}}\psi(2^j t - k), j, k \in \mathbb{Z}\right\}$ is an orthonormal wavelet basis for $L^2(\mathbb{R})$. The function ψ is called wavelet or mother wavelet function. More details about the concept MRA can be find in references [7, 8].

Wavelets basis constitute a family of functions constructed from dilation and translation of the mother wavelet ψ. When the dilation parameter j and the translation parameter k vary, we have the following family of wavelets

$$\psi_{j,k}(t) = 2^{\frac{1}{2}}\psi\left(2^j t - k\right), \ j, k \in \mathbb{Z}. \tag{4.5}$$

As a powerful tool, wavelets have been extensively used in signal processing, numerical analysis, and many other areas. Wavelets permit accurate representation of a variety of functions and operators. Moreover, wavelet basis have been succesfully used to solve different kind of differential and integral equations [6, 17, 23, 1, 28, 30, 24]. In this section we review basic definitions and properties of some commonly used wavelets basis in the field of numerical analysis and computational mathematics.

4.1. Haar wavelets

The orthogonal set of Haar wavelets $h_n(t)$ constitute a set of square waves defined as follows [25]

$$h_n(t) = 2^{\frac{j}{2}}\psi\left(2^j t - k\right), \quad j \geq 0, \quad 0 \leq k < 2^j, \quad n = 2^j + k, \quad n, j, k \in \mathbb{N}, \tag{4.6}$$

where

$$h_0(t) = 1, \quad 0 \leq t < 1, \quad \psi(t) = \begin{cases} 1, & 0 \leq t < \frac{1}{2}, \\ -1, & \frac{1}{2} \leq t < 1. \end{cases} \tag{4.7}$$

Each Haar wavelet $h_n(t)$ has the support $\left[\frac{k}{2^j}, \frac{k+1}{2^j}\right)$, so that it is zero elsewhere in the interval $[0, 1)$. Haar wavelets $h_n(t)$ are pairwise orthonormal in the interval $[0, 1)$ and

$$\int_0^1 h_i(t)h_j(t)dt = \delta_{ij}, \tag{4.8}$$

where δ_{ij} is the Kronecker delta. Any square integrable function $f(t)$ in the interval $[0, 1)$ can be expanded in terms of Haar wavelets as

$$f(t) = c_0 h_0(t) + \sum_{i=1}^{\infty} c_i h_i(t), \tag{4.9}$$

where c_i is given by

$$c_i = \int_0^1 f(t)h_i(t)dt, \tag{4.10}$$

The infinite series in Eq. (4.9) can be truncated after $\hat{m}$ terms, that is

$$f(t) \simeq c_0 h_0(t) + \sum_{i=1}^{\hat{m}-1} c_i h_i(t), \quad i = 2^j + k, \quad 0 \leq k < 2^j, \tag{4.11}$$

rewriting this equation in the vector form we have,

$$f(t) \simeq C^T \Psi(t) = \Psi(t)^T C, \tag{4.12}$$

in which C and $H(t)$ are Haar coefficients and wavelets vectors as

$$C = [c_0, c_1, ..., c_{\hat{m}-1}]^T, \tag{4.13}$$

$$\Psi(t) = [h_0(t), h_1(t), ..., h_{\hat{m}-1}(t)]^T . \tag{4.14}$$

Any two dimensional function $k(s,t) \in L^2[0,1) \times L^2[0,1)$ can be expanded with respect to Haar wavelets as

$$k(s,t) = \Psi^T(t) K \Psi(t), \tag{4.15}$$

where $H(t)$ is the Haar wavelets vector and K is the $\hat{m} \times \hat{m}$ Haar wavelets coefficients matrix with (i,l)-th element can be obtained as

$$k_{ij} = \int_0^1 \int_0^1 k(s,t)\Psi_i(t)\Psi_j(s)dtds, \quad i,j = 1,2,...,\hat{m}. \tag{4.16}$$

4.2. Legendre wavelets

Legendre wavelets $\psi_{mn}(t)$ are defined on the interval $[0,1)$ as [18, 19, 10]

$$\psi_{mn}(t) = \begin{cases} \sqrt{m+\frac{1}{2}}\, 2^{\frac{k+1}{2}} P_m\left(2^{k+1}t - (2n+1)\right) & \frac{n}{2^k} \le t < \frac{n+1}{2^k} \\ 0 & otherwise, \end{cases} \tag{4.17}$$

where $n = 0, 1, ..., 2^k - 1$ and $m = 0, 1, \cdots, M-1$ is the degree of the Legendre polynomials for a fixed positive integer M. Here $P_m(t)$ are the well-known Legendre polynomials of degree m. The Legendre wavelets $\{\psi_{nm}(x) | n = 0, 1, \ldots, 2^k - 1, m = 0, 1, 2, ..., M-1\}$ forms an orthonormal basis for $L^2[0,1]$ with respect to the weight function $w(t) = 1$.

Any square integrable function $f(x)$ defined over $[0, 1)$ can be expanded in terms of the extended Legendre wavelets as

$$f(t) \simeq \sum_{n=0}^{\infty} \sum_{m=0}^{\infty} c_{nm}\psi_{nm}(x), \tag{4.18}$$

where $c_{mn} = (f(t), \psi_{mn}(t))$ and $(.,.)$ denotes the inner product on $L^2[0,1]$. If the infinite series in (4.18) is truncated, then it can be written as

$$f(t) \simeq \sum_{n=0}^{2^k-1} \sum_{m=0}^{M-1} c_{mn}\psi_{mn}(x) = C^T \Psi(t), \tag{4.19}$$

where C and $\Psi(t)$ are $\hat{m} = 2^k M$ column vectors given by

$$C = \left[c_{00}, \ldots, c_{0(M-1)} | c_{10}, \ldots, c_{1(M-1)} |, \ldots, | c_{(2^k-1)0}, \ldots, c_{(2^k-1)(M-1)}\right]^T, \tag{4.20}$$

$$\Psi(t) = \left[\psi_{00}(t), \ldots, \psi_{0(M-1)}(t) | \psi_{10}(t), \ldots, \psi_{1(M-1)}(t) |, \ldots, | \psi_{(2^k-1)0}(t), \ldots, \psi_{(2^k-1)(M-1)}(t)\right]^T .$$

By changing indices in the vectors $\Psi(x)$ and C the series (4.20) can be rewritten as

$$f(t) \simeq \sum_{i=1}^{\hat{m}} c_i \psi_i(t) = C^T \Psi(t), \tag{4.21}$$

where

$$C = [c_1, c_2, ..., c_{\hat{m}}], \quad \Psi(t) = [\psi_1(t), \psi_2(t), ..., \psi_{\hat{m}}(t)], \tag{4.22}$$

and

$$c_i = c_{nm}, \quad \psi_i(x) = \psi_{nm}(x), \quad i = nM + m + 1. \tag{4.23}$$

Similarly, any two dimensional function $k(s,t) \in L^2([0,1] \times [0,1])$ can be expanded into Legendre wavelets basis as

$$k(s,t) \approx \sum_{i=1}^{\hat{m}} \sum_{j=1}^{\hat{m}} k_{ij}\psi_i(s)\psi_j(t) = \Psi^T(s)K\Psi(t), \tag{4.24}$$

where $K = [k_{ij}]$ and $k_{ij} = \Big(\psi_i(s), \Big(u(s,t), \psi_j(t)\Big)\Big)$.

4.3. Chebyshev wavelets

Chebyshev wavelets $\psi_{nm}(x)$ are defined on the interval $[0,1)$ by [9, 15, 14]

$$\psi_{nm}(t) = \begin{cases} 2^{\frac{k+1}{2}}\tilde{T}_m(2^k t - (2n+1)), & \frac{n}{2^k} \le x \le \frac{n+1}{2^k} \\ 0, & otherwise \end{cases}, \tag{4.25}$$

where

$$\tilde{T}_m(t) = \begin{cases} \frac{1}{\sqrt{\pi}}, & m = 0 \\ \sqrt{\frac{2}{\pi}}T_m(t), & m > 0 \end{cases},$$

and $T_m(t)$ are the well-known Chebyshev polynomials of degree m. Chebyshev wavelets $\{\psi_{nm}(x) | n = 0, 1, \ldots, 2^k - 1, m = 0, 1, 2, ..., M-1\}$ form an orthonormal basis for $L^2_{w_n}[0,1]$ with respect to the weight function $w_n(t) = w(2^{k+1}t - (2n+1))$, in which $w(t) = \frac{1}{\sqrt{1-t^2}}$.

By using the orthonormality of the Chebyshev wavelets, any function $f(t)$ over $[0,1)$; square-integrable with respect to the measure $\mathbf{w}(t)dt$; with $\mathbf{w}(t) = w_{nk}(t)$; for $\frac{n}{2^k} \le t \le \frac{n+1}{2^k}$; and $w_{nk}(t) = w(2^{k+1}t - 2n + 1)$; being $w(t) = \frac{1}{\sqrt{1-t^2}}$ can be expanded in terms of the Chebyshev wavelets as

$$f(t) \simeq \sum_{n=0}^{\infty} \sum_{m=0}^{\infty} c_{nm}\psi_{nm}(t), \tag{4.26}$$

where $c_{mn} = (f(t), \psi_{mn}(t))_{w_{nk}}$ and $(.,.)_{w_{nk}}$ denotes the inner product on $L^2_{w_{nk}}[0,1]$. If the infinite series in (4.26) is truncated, then it can be written as

$$f(t) \simeq \sum_{n=0}^{2^k-1} \sum_{m=0}^{M-1} c_{mn}\psi_{mn}(x) = C^T\Psi(t), \tag{4.27}$$

where C and $\Psi(t)$ are $\hat{m} = 2^k M$ column vectors given by

$$C = \Big[c_{00}, \ldots, c_{0(M-1)} | c_{10}, \ldots, c_{1(M-1)} |, \ldots, | c_{(2^k-1)0}, \ldots, c_{(2^k-1)(M-1)}\Big]^T,$$

$$\Psi(x) = \left[\psi_{00}(t), \ldots, \psi_{0(M-1)}(t) | \psi_{10}(t), \ldots, \psi_{1(M-1)}(t) |, \ldots, | \psi_{(2^k-1)0}(t), \ldots, \psi_{(2^k-1)(M-1)}(t)\right]^T. \quad (4.28)$$

By changing indices in the vectors $\Psi(t)$ and C the series (4.28) can be rewritten as

$$f(t) \simeq \sum_{i=1}^{\hat{m}} c_i \psi_i(t) = C^T \Psi(t), \quad (4.29)$$

where

$$C = [c_1, c_2, ..., c_{\hat{m}}], \quad \Psi(x) = [\psi_1(x), \psi_2(x), ..., \psi_{\hat{m}}(x)], \quad (4.30)$$

and

$$c_i = c_{nm}, \quad \psi_i(t) = \psi_{nm}(t), \quad i = nM + m + 1.$$

Similarly, any two dimensional function $k(s,t) \in L^2_{\mathbf{w}\bigotimes\mathbf{w}}([0,1] \times [0,1])$ can be expanded into Chebyshev wavelets basis as

$$k(s,t) \approx \sum_{i=1}^{\hat{m}} \sum_{j=1}^{\hat{m}} k_{ij} \psi_i(s) \psi_j(t) = \Psi^T(s) K \Psi(t), \quad (4.31)$$

where $K = [k_{ij}]$ is an $\hat{m} \times \hat{m}$ matrix and $k_{ij} = \left(\psi_i(s), \left(k(s,t), \psi_j(t)\right)_{w_{nk}}\right)_{w_{nk}}$.

4.4. Second kind Chebyshev wavelets

Second kind Chebyshev wavelets $\psi_{nm}(t)$ are defined on the interval $[0,1)$ by [29]

$$\psi_{nm}(t) = \begin{cases} \sqrt{\frac{2}{\pi}} 2^{\frac{k+1}{2}} U_m\left(2^{k+1}t - 2n - 1\right), & \frac{n}{2^k} \le x \le \frac{n+1}{2^k} \\ 0, & otherwise, \end{cases}, \quad (4.32)$$

where $U_m(t)$ is the second kind Chebyshev polynomials of degree m, given by

$$U_m(t) = \frac{\sin((m+1)\theta)}{\sin(\theta)}, \quad t = \cos(\theta). \quad (4.33)$$

The second kind Chebyshev wavelets $\{\psi_{nm}(t) | n = 0, 1, \ldots, 2^k - 1, m = 0, 1, 2, ..., M-1\}$ forms an orthonormal basis for $L^2_{w_{nk}}[0,1]$ with respect to the weight function $w_{nk}(t) = w\left(2^{k+1}t - 2n - 1\right)$, in which $w(t) = \sqrt{1-t^2}$. By using the orthonormality of the second kind Chebyshev wavelets, any square integrable function $f(t)$ defined over $[0,1)$ can be expanded in terms of the second kind Chebyshev wavelets as

$$f(t) \simeq \sum_{n=0}^{\infty} \sum_{m=0}^{\infty} c_{nm} \psi_{nm}(t), \quad (4.34)$$

where $c_{mn} = (f(t), \psi_{mn}(t))_{w_{nk}}$ and $(.,.)_{w_{nk}}$ denotes the inner product on $L^2_{w_{nk}}[0,1]$. If the infinite series in (4.42) is truncated, then it can be written as

$$f(t) \simeq \sum_{n=0}^{2^k-1} \sum_{m=0}^{M-1} c_{mn}\psi_{mn}(x) = C^T\Psi(t), \tag{4.35}$$

where C and $\Psi(t)$ are $\hat{m} = 2^k M$ column vectors given by

$$C = \left[c_{00}, \ldots, c_{0(M-1)}|c_{10}, \ldots, c_{1(M-1)}|, \ldots, |c_{(2^k-1)0}, \ldots, c_{(2^k-1)(M-1)}\right]^T,$$

$$\Psi(x) = \left[\psi_{00}(t), \ldots, \psi_{0(M-1)}(t)|\psi_{10}(t), \ldots, \psi_{1(M-1)}(t)|, \ldots, |\psi_{(2^k-1)0}(t), \ldots, \psi_{(2^k-1)(M-1)}(t)\right]^T. \tag{4.36}$$

By changing indices in the vectors $\Psi(t)$ and C the series (4.36) can be rewritten as

$$f(t) \simeq \sum_{i=1}^{\hat{m}} c_i\psi_i(t) = C^T\Psi(t), \tag{4.37}$$

where

$$C = [c_1, c_2, ..., c_{\hat{m}}], \quad \Psi(x) = [\psi_1(x), \psi_2(x), ..., \psi_{\hat{m}}(x)], \tag{4.38}$$

and

$$c_i = c_{nm}, \quad \psi_i(t) = \psi_{nm}(t), \quad i = nM + m + 1. \tag{4.39}$$

Similarly, any two dimensional function $k(s,t) \in L^2([0,1] \times [0,1])$ can be expanded into second kind Chebyshev wavelets basis as

$$k(s,t) \approx \sum_{i=1}^{\hat{m}} \sum_{j=1}^{\hat{m}} k_{ij}\psi_i(s)\psi_j(t) = \Psi^T(s)K\Psi(t), \tag{4.40}$$

where $K = [k_{ij}]$ and $k_{ij} = \left(\psi_i(s), \left(u(s,t), \psi_j(t)\right)_{w_{nk}}\right)_{w_{nk}}$.

4.5. CAS Wavelet

CAS wavelets $\psi_{nm}(t)$ are defined on the interval $[0,1)$ as follows [26]

$$\psi_{mn}(t) = \begin{cases} 2^{\frac{k}{2}} CAS_m\left(2^k t - n + 1\right), & \frac{n-1}{2^k} \leq t < \frac{n-1}{2^k}, \\ 0, & otherwise \end{cases} \tag{4.41}$$

where $CAS_m(t) = \cos(2m\pi t) + \sin(2m\pi t)$. The set of CAS wavelets $\{\psi_{nm}(t)|n = 0, 1, \ldots, 2^k - 1, m = -M, ...0, 1, 2, ..., M-1\}$ forms an orthonormal basis for $L^2([0,1))$. This implies that any square inegrable function $f(t)$ defined over $[0,1)$ can be expanded in terms of the CAS wavelets as

$$f(t) \simeq \sum_{n=0}^{\infty} \sum_{m\in\mathbb{Z}}^{\infty} c_{nm}\psi_{nm}(t), \tag{4.42}$$

where $c_{mn} = (f(t), \psi_{mn}(t))$ and $(.,.)$ is the inner product on $L^2[0,1]$. If the infinite series in (4.42) is truncated, then it can be written as

$$f(t) \simeq \sum_{n=0}^{2^k-1} \sum_{m=-M}^{M} c_{mn}\psi_{mn}(x) = C^T\Psi(t), \tag{4.43}$$

where C and $\Psi(t)$ are $\hat{m} = 2^k(2M+1)$ column vectors given by

$$C = \left[c_{0,-M}, \ldots, c_{0,M}, \ldots, c_{1,-M}, \ldots, c_{1,M}, \ldots, c_{(2^k-1),-M}, \ldots, c_{(2^k-1),M}\right]^T,$$

$$\Psi(t) = \left[\psi_{0,-M}, \ldots, \psi_{0,M}, \ldots, \psi_{1,-M}, \ldots, \psi_{1,M}, \ldots, \psi_{(2^k-1),-M}, \ldots, \psi_{(2^k-1),M}\right]^T, \tag{4.44}$$

By changing indices in the vectors $\Psi(t)$ and C the series (4.44) can be rewritten as

$$f(t) \simeq \sum_{i=1}^{\hat{m}} c_i\psi_i(t) = C^T\Psi(t), \tag{4.45}$$

where

$$C = [c_1, c_2, ..., c_{\hat{m}}], \quad \Psi(x) = [\psi_1(x), \psi_2(x), ..., \psi_{\hat{m}}(x)], \tag{4.46}$$

and

$$c_i = c_{nm}, \quad \psi_i(t) = \psi_{nm}(t), \quad i = (n-1)(2M+1) + M + m + 1. \tag{4.47}$$

Moreover, any two dimensional function $k(s,t) \in L^2([0,1] \times [0,1])$ can be expanded into second kind Chebyshev wavelets basis as

$$k(s,t) \approx \sum_{i=1}^{\hat{m}} \sum_{j=1}^{\hat{m}} k_{ij}\psi_i(s)\psi_j(t) = \Psi^T(s)K\Psi(t), \tag{4.48}$$

where $K = [k_{ij}]$ and $k_{ij} = \left(\psi_i(s), \left(u(s,t), \psi_j(t)\right)_{w_{nk}}\right)_{w_{nk}}$.

5. Operational matrix of the fractional integration

The wavelets basis $\Psi(t)$ can be expressed in the $\hat{m}$-dimensional BPFs. Next theorem describe the relation between the wavelet basis $\Psi(t)$ and BPFs $B(t)$.

Theorem 5.1. *Let $\Psi(t)$ and $B(t)$ be the $\hat{m}$-dimensional wavelets and BPFs vector respectively, the vector $\Psi(t)$ can be expanded by BPFs vector $B(t)$ as*

$$\Psi(t) \simeq QB(t), \tag{5.1}$$

where Q is an $\hat{m} \times \hat{m}$ block matrix and

$$Q_{ij} = \psi_i\left(\frac{2j-1}{2\hat{m}}\right), \qquad i, j = 1, 2, ..., \hat{m}. \tag{5.2}$$

Proof. Let $\psi_i(t), i = 1, 2, ..., \hat{m}$ be the i-th element of the wavelets vector $\psi(t)$. Expanding $\psi_i(t)$ into an $\hat{m}$-term vector of BPFs, we have

$$\psi_i(t) \simeq \sum_{k=1}^{\hat{m}} Q_{ik} b_k(t), \qquad i = 1, 2, ..., \hat{m}, \tag{5.3}$$

taking the collocation points $\eta_j = \frac{2j-1}{2\hat{m}}$ and evaluating relation (5.3) we get

$$\psi_i(\eta_j) \simeq \sum_{k=1}^{\hat{m}} Q_{ik} b_k(\eta_j) = Q_{ij}, \qquad i, j = 1, 2, ..., \hat{m}, \tag{5.4}$$

and this prove the desired result. □

Now we derive the operational matrices of integration for the wavelets vector $\Psi(t)$. A general procedures for forming these matrix will be described in next theorem. First, we remind some useful results for BPFs.

Lemma 5.2. *[12] Let $B(t)$ be the $\hat{m}$-dimensional BPFs vector defined in (3.7), then integration of this vector can be derived as*

$$\int_0^t B(s)ds \simeq PB(t), \tag{5.5}$$

where P is called the operational matrix of integration for BPFs and is given by

$$P = \frac{h}{2} \begin{bmatrix} 1 & 2 & 2 & \dots & 2 \\ 0 & 1 & 2 & \dots & 2 \\ 0 & 0 & 1 & \vdots & \vdots \\ \vdots & \vdots & \vdots & \ddots & 2 \\ 0 & 0 & 0 & \dots & 1 \end{bmatrix}_{\hat{m}\times\hat{m}}. \tag{5.6}$$

Lemma 5.3. *[12] Let $B(t)$ be the $\hat{m}$-dimensional BPFs vector defined in (3.7), then integration of this vector can be derived as*

$$J^\alpha B(t) = P^\alpha B(t), \tag{5.7}$$

where P^α is called the operational matrix of integration for BPFs and is given by

$$P^\alpha = \frac{h^\alpha}{\Gamma(\alpha+2)} \begin{bmatrix} 1 & \xi_1 & \xi_2 & \dots & \xi_{m-1} \\ 0 & 1 & \xi_1 & \dots & \xi_{m-2} \\ 0 & 0 & 1 & \dots & \xi_{m-3} \\ 0 & 0 & 0 & \ddots & \vdots \\ 0 & 0 & 0 & 0 & 1 \end{bmatrix}. \tag{5.8}$$

Theorem 5.4. *Suppose $\Psi(t)$ be an $\hat{m}$-dimensional wavelets vector, the integral of this vector can be derived as*

$$\int_0^t \Psi(s)ds \simeq QPQ^{-1}\Psi(t) = \Lambda\Psi(t), \tag{5.9}$$

where Q is introduced in (5.1) and P is the operational matrix of integration for BPFs derived in (5.6).

Proof. Let $\Psi(t)$ be the wavelets vector, by using Theorem 5.1 and Lemma 5.3 we have

$$\int_0^t \Psi(s)ds \simeq \int_0^t QB(s)ds = Q\int_0^t B(s)ds = QPB(t), \tag{5.10}$$

now theorem 5.1 results

$$\int_0^t \Psi(s)ds \simeq QPB(t) = QPQ^{-1}\Psi(t) = \Lambda\Psi(t), \tag{5.11}$$

by using this identity we obtain the desired result. □

Theorem 5.5. *Let $\Psi(t)$ be the an $\hat{m}$-dimensional wavelets vector, the operational matrix of the fractional order integration for $\Psi(t)$ can be derived as*

$$J^\alpha\Psi(t) = QP^\alpha Q^{-1}\Psi(t) = \Lambda^\alpha\Psi(t), \tag{5.12}$$

where Λ^α is called the operational matrix of second kind Chebyshev wavelets, Q is the matrix introduced in (5.1) and P^α is the operational matrix of fractional integration for BPFs derived in (5.8).

Proof. By using Theorem 5.1 we have

$$J^\alpha\Psi(t) = J^\alpha Q\Phi(t) = QF^\alpha\Phi(t) = QF^\alpha Q^{-1}\Psi(t) = P^\alpha\Psi(t), \tag{5.13}$$

so, the second kind Chebyshev wavelet operational matrix of the fractional order integration P^α is given by

$$P^\alpha = QF^\alpha Q^{-1}. \tag{5.14}$$

and this completes the proof. □

6. Method of solution

In this section, a collocation method based on BPFs and wavelet basis is presented for approximating solution of FIDE with a weakly singular kernel defined in (1.1). The presented technique can be applied by using BPFs and all wavelets basis introduced in the previous section. From now

on by $\Phi(t)$ we mean BPFs or any introduced wavelet basis vector. Consider FIDE with a weakly singular kernel (1.1), we first approximate functions $D^{\alpha}_{*}u(t)$ and $k(t,s)$ as

$$D^{\alpha}_{*}u(t) = C^{T}\Phi(t), \qquad k(t,s) = \Phi(t)^{T}K\Phi(t), \tag{6.1}$$

where $\Phi(t)$ can be BPFs or wavelet vector, C is an unknown vector and K is a known coefficient matrix of $k(t,s)$ corresponding to the basis vector $\Phi(t)$. By using the properties of Caputo fractional operators D^{α}_{*} and operational matrix of fractional oreder on the basis vector $\Phi(t)$ we get

$$u(t) = J^{\alpha}\left(D^{\alpha}_{*}u(t)\right) = C^{T}J^{\alpha}\Phi(t) = C^{T}P^{\alpha}\Phi(t), \tag{6.2}$$

substituting Eqs. (6.1) and (6.2) into Eq. (1.1), we have

$$\begin{aligned} C^{T}\Phi(t) &= F^{T}\Phi(t) + \int_{0}^{t}\frac{C^{T}P^{\alpha}\Phi(s)ds}{(t-s)^{\beta}} + \int_{0}^{1}\Phi(t)^{T}K\Phi(s)C^{T}P^{\alpha}\Phi(s)ds \\ &= F^{T}\Phi(t) + C^{T}P^{\alpha}\int_{0}^{t}\frac{\Phi(s)ds}{(t-s)^{\beta}} + \Phi(t)^{T}K\left(\int_{0}^{1}\Phi(s)\Phi(s)^{T}ds\right)(P^{\alpha})^{T}C \\ &= F^{T}\Phi(t) + C^{T}P^{\alpha}\int_{0}^{t}\frac{\Phi(s)ds}{(t-s)^{\beta}} + h\Phi(t)^{T}KQ\left(P^{\alpha}Q\right)^{T}C, \end{aligned} \tag{6.3}$$

and for the case that $\Phi(t)$ is the BPFs vector, the matrix $Q = I_{\hat{m}}$ will be the identity matrix. Now we consider the weakly singular integral $\int_{0}^{t}\frac{\Phi(s)ds}{(t-s)^{\beta}}$. For $(i-1)h \le t \le ih$, this singular integral can be approximated as

$$\int_{0}^{t}\frac{\Phi(s)ds}{(t-s)^{\beta}} = Q\int_{0}^{t}\frac{B(s)ds}{(t-s)^{\beta}} = Q\left[\int_{0}^{h}\frac{ds}{(t-s)^{\beta}}, \int_{h}^{2h}\frac{ds}{(t-s)^{\beta}}..., \int_{(i-1)h}^{t}\frac{ds}{(t-s)^{\beta}}, 0, ..., 0\right]^{T}$$

$$= Q\left[\frac{t^{-\beta+1}-(t-h)^{-\beta+1}}{\beta-1}, \frac{(t-h)^{-\beta+1}-(t-2h)^{-\beta+1}}{\beta-1}, ..., \frac{(t-(i-1)h)^{-\beta+1}}{\beta-1}, 0, ..., 0\right]^{T} = V(t). \tag{6.4}$$

Substituting the vector $V(t)$ in Eq. (6.3), we get

$$C^{T}\Phi(t) = F^{T}\Phi(t) + C^{T}P^{\alpha}V(t) + h\Phi(t)^{T}KQ\left(P^{\alpha}Q\right)^{T}C, \tag{6.5}$$

by taking the appropriate collocation points $t_i, i = 1, ..., \hat{m}$ and evaluating Eq. (6.5) we obtain the following linear system of algebraic equations for the unknown vector C

$$C^{T}\Phi(t_i) - F^{T}\Phi(t_i) - C^{T}P^{\alpha}V(t_i) - h\Phi(t_i)^{T}KQ\left(P^{\alpha}Q\right)^{T}C = 0, \quad i = 0, 1, ..., m. \tag{6.6}$$

By solving this linear system and determining vector C, we can approximate solution of fractional integro-differential equation with a weakly singular kernel (1.1) by substituting the obtained vector C in Eq. (6.2).

7. Estimation of the error function

Suppose $u(t)$ is the exact solution of (1.1) and $u_{\hat{m}}(t)$ is the approximate solution for $u(t)$. Here, we introduce a process for estimating the error of approximate solution, i. e. $e_{\hat{m}}(t) = u(t) - u_{\hat{m}}(t)$. First, by using definition of fractional integration operator J^{α}, the solution of FIDE with a weakly singular kernel (1.1) can be written as

$$u(s) = \frac{1}{\Gamma(\alpha)} \int_0^t \frac{f(\tau)d\tau}{(t-\tau)^{1-\alpha}} + \frac{1}{\Gamma(\alpha)} \int_0^t \frac{1}{(t-\tau)^{1-\alpha}} \int_0^\tau \frac{u(s)dsd\tau}{(\tau-s)^{\beta}} + \frac{1}{\Gamma(\alpha)} \int_0^t \int_0^1 \frac{k(s,\tau)u(s)}{(t-\tau)^{1-\alpha}} dsd\tau \quad (7.1)$$

now consider the perturbation function $r_{\hat{m}}(t)$ that depends only on $u_{\hat{m}}(t)$ as

$$r_{\hat{m}}(t) = \frac{1}{\Gamma(\alpha)} \int_0^t \frac{f(\tau)d\tau}{(t-\tau)^{1-\alpha}} + \frac{1}{\Gamma(\alpha)} \int_0^t \frac{1}{(t-\tau)^{1-\alpha}} \int_0^\tau \frac{u_{\hat{m}}(s)dsd\tau}{(\tau-s)^{\beta}}$$

$$+\frac{1}{\Gamma(\alpha)} \int_0^t \frac{1}{(t-\tau)^{1-\alpha}} \int_0^1 k(s,\tau)u_{\hat{m}}(s)dsd\tau - u_{\hat{m}}(t), \quad (7.2)$$

subtracting (7.2) from (7.1) we obtain

$$e_{\hat{m}}(t) = r_{\hat{m}}(t) + \frac{1}{\Gamma(\alpha)} \int_0^t \frac{1}{(t-\tau)^{1-\alpha}} \int_0^\tau \frac{e_{\hat{m}}(s)dsd\tau}{(\tau-s)^{\beta}} + \frac{1}{\Gamma(\alpha)} \int_0^t \frac{1}{(t-\tau)^{1-\alpha}} \int_0^1 k(s,\tau)e_{\hat{m}}(s)dsd\tau,$$

this is a fractional integral equations in which the error function $e_{\hat{m}}(t)$ is unknown. Obviously, we can apply the proposed collocation method as given in previous section for this system to find an approximation of the error function $e_{\hat{m}}(t)$.

8. Numerical results and discussion

In this section, we will present numerical experiments derived by using collocation method described in Section 6. The results of the proposed method for different kind of wavelet basis are also compared with exact solution. All computations are performed by Maple 17 with 20 digits precision and Intel Core 2 Duo CPU 2.50 GHz package.

Example 8.1. Let us consider the following FIDE with weakly singular kernel [13]

$$D_*^{0.25}u(t) = f(t) + \frac{1}{2} \int_0^t \frac{u(s)ds}{(t-s)^{\frac{1}{2}}} + \frac{1}{3} \int_0^1 (t-s)u(s),$$

with the initial condition $u(0) = 0$ and

$$f(t) = \frac{\Gamma(3)}{\Gamma(2.75)} t^{1.75} + \frac{\Gamma(4)}{\Gamma(3.75)} t^{2.75} - \frac{\sqrt{\pi}\Gamma(3)}{2\Gamma(3.5)} t^{2.5} - \frac{\sqrt{\pi}\Gamma(4)}{2\Gamma(4.5)} t^{3.5} - \frac{7t}{36} + \frac{3}{20}.$$

The exact solution of this equation is $u(t) = t^2 + t^3$. The presented collocation method in section 6 with wavelet and BPFs basis is used for approximating solution of this FIDE with weakly singular

kernel. Table 1 presents the maximum absolute error of the numerical results derived by different wavelet basis and BPFs for various values of $\hat{m}$. As numerical results in Table 1 reveal, the LW, CHW and SKCHW have same convergence behavior and they are more accurate in comparison with other wavelets basis and BPFs. Moreover, computational time of different wavelet and BPFs methods for $\hat{m} = 64$ are listed in Table 2. From this Table it is possible to see that the computational time of CASW is higher than other kind of used basis function and BPFs has the minimum computational time.

Table 1: Comparison of the maximum absolute error for different wavelet basis and various values of $\hat{m}$.

	$\hat{m} = 24$	$\hat{m} = 48$	$\hat{m} = 64$
BPFs	1.22×10^{-1}	5.14×10^{-2}	4.01×10^{-2}
HW	2.23×10^{-1}	4.32×10^{-2}	3.82×10^{-2}
LW	5.21×10^{-3}	1.20×10^{-3}	1.13×10^{-3}
CHW	4.86×10^{-3}	1.18×10^{-3}	1.12×10^{-3}
SKCHW	5.25×10^{-3}	1.42×10^{-3}	1.12×10^{-3}
CASW	2.53×10^{-1}	5.50×10^{-2}	1.52×10^{-2}

Table 2: Comparison of computational time (in seconds) for different wavelet basis and $\hat{m} = 64$.

	BPFs	HW	LW	CHW	SKCHW	CASW
CPU time (sec)	135.695	1380.141	140.436	148.217	142.176	187.042

Example 8.2. Consider the FIDE with weakly singular kernel [13]

$$D_*^{0.15}u(t) = f(t) + \frac{1}{4}\int_0^t \frac{u(s)ds}{(t-s)^{\frac{1}{2}}} + \frac{1}{7}\int_0^1 e^{t+s}u(s),$$

in which $u(0) = 0$ and

$$f(t) = \frac{\Gamma(3)}{\Gamma(2.85)}t^{1.85} - \frac{\Gamma(2)}{\Gamma(1.85)}t^{0.85} - \frac{\sqrt{\pi}\Gamma(3)}{4\Gamma(3.5)}t^{2.5} + \frac{\sqrt{\pi}\Gamma(2)}{4\Gamma(2.5)}t^{1.5} - \frac{e^{t+1} - 3e^t}{7}.$$

In this problem the exact solution of this equation is $u(t) = t^2 - t$. We have solved this FIDE with weakly singular kernel by using the wavelet and BPFs collocation methods. The maximum absolute error of the numerical results derived by wavelet basis and BPFs collocation method for various values of $\hat{m}$ are presented in Table 3. Similar to the previous example, the numerical results obtained by LW, CHW and SKCHW basis are more accurate in compare to othe basis. Moreover, Table 3 indicate that the LW, CHW and SKCHW have same convergence behavior as BPFs and HW have same. Computational time for different wavelet and BPFs basis with $\hat{m} = 64$ are listed in Table 2. From this Table it is possible to see that the computational time of CASW is higher than other kind of basis functions and BPFs has the minimum computational time.

Table 3: Comparison of the maximum absolute error for different wavelet basis and various values of $\hat{m}$.

	$\hat{m} = 24$	$\hat{m} = 48$	$\hat{m} = 64$
BPFs	2.62×10^{-2}	1.24×10^{-2}	8.41×10^{-3}
HW	1.16×10^{-2}	1.21×10^{-2}	8.82×10^{-3}
LW	2.35×10^{-3}	1.14×10^{-3}	1.14×10^{-3}
CHW	3.51×10^{-3}	1.16×10^{-3}	2.24×10^{-3}
SKCHW	3.27×10^{-3}	2.64×10^{-3}	2.11×10^{-3}
CASW	5.43×10^{-2}	3.11×10^{-2}	2.54×10^{-2}

Table 4: Comparison of computational time (in seconds) for different wavelet basis and $\hat{m} = 64$.

	BPFs	HW	LW	CHW	SKCHW	CASW
CPU time (sec)	140.688	142.146	141.235	147.249	148.698	194.771

Example 8.3. Let us consider the following fractional order integro-differential equation with a weakly singular kernel [13]

$$D_*^{\alpha} u(t) = f(t) + \int_0^t \frac{u(s)ds}{(t-s)^{\frac{1}{2}}} + \int_0^1 (t + sin(s))u(s),$$

where $u(0) = 0$ and

$$f(t) = 2t - \frac{\sqrt{\pi}\Gamma(3)}{2\Gamma(3.5)} t^{2.5} - \frac{t}{3} - \cos(1) - 2\sin(1) + 2.$$

When $\alpha = 1$, the exact solution of this fractional integro-differential equation is $u(t) = t^2$. The proposed collocation method are used for solving this FIDE for various values of α and different kind wavelet basis. The maximum absolute error of numerical solutions with $\alpha = 1$ are tabulated in Table 5. From this Table, we infer that numerical solutions derived by BPFs and all wavelet basis converge to the exact solution. Moreover, numerical solutions for $\alpha = 0.85$ and $\alpha = 0.95$ are listed in Tables 6 and 7. As it is obvious from Tables 6 and 7 the numerical solutions converge to the exact solution $u(t) = t^2$ as α is close to 1. Table 8 displays the comparison between the computational time of BPFs and different wavelet basis for $\alpha = 1$ and $\hat{m} = 64$. As can be observed from this Table, the computational time of BPFs method is minimum and computational time of CASW method is higher than other kind of basis functions.

9. Discussion and conclusion

This paper deals with a comparitive study of wavelet collocation methods for numerical solution of fractional order integro-differential equation with a weakly singular kernel. The numerical results derived by different kind of wavelets basis are also compared with the BPFs collocation method. A comparison is made between computational time of the proposed collocation methods for BPFs and different kind of wavelet basis. The comparison of the experimental results highlighted that:

Table 5: Comparison of the maximum absolute error for different wavelet basis and various values of $\hat{m}$.

	$\hat{m} = 24$	$\hat{m} = 48$	$\hat{m} = 64$
BPFs	3.34×10^{-1}	3.14×10^{-2}	1.84×10^{-2}
HW	6.84×10^{-1}	3.43×10^{-2}	2.88×10^{-2}
LW	5.77×10^{-3}	4.87×10^{-3}	2.68×10^{-3}
CHW	4.05×10^{-3}	1.28×10^{-3}	1.32×10^{-3}
SKCHW	5.69×10^{-3}	4.66×10^{-3}	2.34×10^{-3}
CASW	2.43×10^{-1}	7.50×10^{-2}	2.25×10^{-2}

Table 6: The numerical results derived by different wavelet basis for $\alpha = 0.85$ and $\hat{m} = 64$.

t	BPFs	HW	LW	CHW	SKCHW	CASW
0.1	0.075912	0.075912	0.074556	0.074556	0.074556	0.082991
0.3	0.322010	0.322010	0.314696	0.314696	0.314696	0.289446
0.5	1.402528	1.402528	1.402275	1.402274	1.402274	1.527805
0.7	1.239159	1.239159	1.254223	1.254223	1.254223	1.294679
0.9	1.995424	1.995424	2.002114	2.002115	2.002114	1.966650

Table 7: The numerical results derived by different wavelet basis for $\alpha = 0.95$ and $\hat{m} = 64$.

t	BPFs	HW	LW	CHW	SKCHW	CASW
0.1	0.020154	0.020154	0.019664	0.019664	0.019664	0.022894
0.3	0.131961	0.131961	0.128306	0.128306	0.128306	0.115236
0.5	0.659830	0.659831	0.659685	0.659685	0.659685	0.731165
0.7	0.618552	0.618552	0.626625	0.626625	0.626625	0.648190
0.9	1.019279	1.019279	1.022773	1.022773	1.022773	1.004034

Table 8: Comparison of computational time (in seconds) for $\alpha = 1$ and $\hat{m} = 64$.

	BPFs	HW	LW	CHW	SKCHW	CASW
CPU time (sec)	155.429	152.397	162.587	164.239	170.234	210.537

1. The proposed collocation methods with BPFs and wavelet basis are simple and effective for numerical solution of fractional order integro-differential equation with a weakly singular kernel.

2. The numerical results obtained by LW, CHW and SKCHW basis are more accurate comparing with BPFs and the other kind of wavelet basis considered in this paper. In fact, being the BPFs linear functions, as expected they can capture only a first approximation of the numerical solution.

3. The presented collocation methods with LW, CHW and SKCHW have same convergence behavior as BPFs and HW have same convergence behavior.

4. The computational time of CASW is more than BPFs and other kind of wavelet basis. Moreover, the BPFs collocation method has the minimum computational time. In fact, according to theorems 5.4 and 5.5, the operational matrices of wavelets are obtained by a matrix product with the operational matrix of BPFs thus implying a greater computational time.

5. In general, the LW collocation method is the best one for solving fractional order integro-differential equation with a weakly singular kernel.

6. The examples given in section 8 show that, when the analytical solution is a polynomial, then Legendre polynomials and other kind of polynomial based wavelets are good methods of approximation. However in some more general case when the solution is a more general function then it would be more expedient to use different kind of wavelets more similar to the solution.

References

[1] S. Arbabi, A. Nazari, and M.T. Darvishi, A two-dimensional Haar wavelets method for solving systems of PDEs. *Appl. Math. Comput.,* **292** (2017), 33–46.

[2] C. Cattani, *Local Fractional Calculus on Shannon Wavelet Basis,* Nonlinear Physical Science, 2015.

[3] C. Cattani, Shannon wavelets for the solution of integro-differential equations, *Math. Probl. Eng.,* **2010** (2010), doi:10.1155/2010/408418.

[4] C. Cattani, Shannon wavelets theory, *Math. Probl. Eng.,* **2008** (2008), doi:10.1155/2008/164808.

[5] C. Cattani and A. Kudreyko, Harmonic wavelet method towards solution of the Fredholm type integral equations of the second kind, *Appl. Math. Comput.,* **215**(12) (2010), 4164–4171.

[6] I. Celik, Chebyshev Wavelet collocation method for solving generalized BurgersHuxley equation, *Math. Methods Appl. Sci.,* **39**(3) (2016), 366–377.

[7] C.K. Chui, *An Introduction to Wavelets, (Wavelet Analysis and Its Applications),* vol. 1, Elsevier Press, Amsterdam 1992.

[8] E. Hernandez and G. Weiss, *A First Course on Wavelets, Studies in Advanced Mathematics,* CRC Press, Boca Raton, FL, 1996.

[9] M.H. Heydari, M.R. Hooshmandasl, F.M. Ghaini and C. Cattani, Wavelets method for solving fractional optimal control problems, *Appl. Math. Comput.,* **286** (2016) 139–154.

[10] M.H. Heydari, M.R. Hooshmandasl and F. Mohammadi, Two-Dimensional Legendre Wavelets for Solving Time-Fractional Telegraph Equation, *Adv. Appl. Math. Mech.,* **6**(2) (2014), 247–260.

[11] M.R. Hooshmandasl, M.H. Heydari and C. Cattani, Numerical solution of fractional sub-diffusion and time-fractional diffusion-wave equations via fractional-order Legendre functions, *Eur. Phys. J. Plus,* (2016) 131–268, doi:10.1140/epjp/i2016-16268-2.

[12] A. Kilicman and Z.A. Zhour, Kronecker operational matrices for fractional calculus and some applications, *Appl. Math. Comput.,* **187**(1) (2007), 250–65.

[13] Y. Li, Solving a nonlinear fractional differential equation using Chebyshev wavelets, *Commun. Nonlinear Sci. Numer. Simul.* **15** (2010), 2284–2292.

[14] F. Mohammadi, A Chebyshev wavelet operational method for solving stochastic Volterra-Fredholm integral equations, *Int. J. Appl. Math. Res.,* **4**(2) (2015), 217–227.

[15] F. Mohammadi, A wavelet-based computational method for solving stochastic Ito-Volterra integral equations, *J. Comput. Phys.,* **298** (2015), 254–265.

[16] F. Mohammadi, Numerical solution of Bagley-Torvik equation using Chebyshev wavelet operational matrix of fractional derivative, *Int. J. Adv. Appl. Math. Mech.,* **2**(1) (2014), 83–91.

[17] F. Mohammadi, Numerical solution of stochastic Ito-Volterra integral equations using Haar wavelets, *Numer. Math., Theory Methods Appl.,* **9**(3) (2016), 416–431.

[18] F. Mohammadi and M.M. Hosseini, A new Legendre wavelet operational matrix of derivative and its applications in solving the singular ordinary differential equations, *J. Franklin Inst.,* **348**(8) (2011), 1787–1796.
[19] F. Mohammadi and M.M. Hosseini, Legendre wavelet method for solving linear stiff systems, *Journal of Advanced Research in Differential Equations,* **2**(1) (2010), 47–57.
[20] S.T. Mohyud-Din, A. Ali and B. Bin-Mohsin, On biological population model of fractional order, *Int. J. Biomath.,* **9** (2016), doi:10.1142/S1793524516500704.
[21] S.T. Mohyud-Din, A. Waheed and M.M. Rashidi, A study of nonlinear age-structured population models, *Int. J. Biomath.,* **9** (2016), doi:10.1142/S1793524516500911.
[22] I. Podlubny, *Fractional Differential Equations,* Academic Press, San Diego, 1999.
[23] P. Rahimkhani, Y. Ordokhani, and E. Babolian, A new operational matrix based on Bernoulli wavelets for solving fractional delay differential equations, *Numer. Algorithms,* **74**(1) (2017), 223–245.
[24] S.S. Ray and A.K. Gupta, Numerical solution of fractional partial differential equation of parabolic type with Dirichlet boundary conditions using Two-dimensional Legendre wavelets method, *Journal of Computational and Nonlinear Dynamics,* **11**(1) (2016), doi:10.1115/1.4028984.
[25] H. Saeedi, Application of the haar wavelets in solving nonlinear fractional Fredholm intergro-differential equations, *J. Mahani Math. Res. Cent.,* **2**(1) (2012), 15–28.
[26] H. Saeedi and M. Mohseni Moghadam, Numerical solution of nonlinear Volterra integro-differential equations of arbitrary order by CAS wavelets, *Commun. Nonlinear Sci. Numer. Simul.,* **16**(3) (2011), 1216–1226.
[27] H. Saeedi, M. Mohseni Moghadam , M. Mollahasani and G.N. Chuev, A CAS wavelet method for solving nonlinear Fredholm integro-differential equations of fractional order. *Commun. Nonlinear. Sci. Numer. Simul.,* **16**(3) (2011), 1154–63
[28] S.C. Shiralashetti and A. B. Deshi, An efficient Haar wavelet collocation method for the numerical solution of multi-term fractional differential equations, *Nonlinear Dyn.,* **83**(2) (2016), 293–303.
[29] Y. Wang and Q. Fan, The second kind Chebyshev wavelet method for solving fractional differential equations, *Appl. Math. Comput.,* **218**(17) (2012), 8592–8601.
[30] Y. Wang and L. Zhu, SCW method for solving the fractional integro-differential equations with a weakly singular kernel, *Appl. Math. Comput.,* **275** (2016), 72–80.
[31] X.J. Yang, J.T. Machado, D. Baleanu and C. Cattani, On exact traveling-wave solutions for local fractional Korteweg-de Vries equation, *Chaos*, **26**(8) (2016), doi: 10.1063/1.4960543.
[32] X.J. Yang, J.T. Machado and J. Hristov, Nonlinear dynamics for local fractional Burgers equation arising in fractal flow, *Nonlinear Dyn.,* **84**(1) (2016), 3–7.
[33] X.J. Yang, J.T. Machado and H.M. Srivastava, A new numerical technique for solving the local fractional diffusion equation: two-dimensional extended differential transform approach, *Appl. Math. Comput.,* **274** (2016), 143–151.
[34] X.J. Yang, H.M. Srivastava and C. Cattani, Local fractional homotopy perturbation method for solving fractal partial differential equations arising in mathematical physics, *Rom. Rep. Phys.,* **67**(3) (2015), 752–761.